Frequency Mixing Using Electromagnetically Induced Transparency in Cold Atoms

Danielle A. Braje,* Vlatko Balić, Sunil Goda, G. Y. Yin, and S. E. Harris
Edward L. Ginzton Laboratory, Stanford University, Stanford, California 94305, USA
(Received 17 June 2004; published 29 October 2004)

We report the first experimental demonstration of four-wave mixing using electromagnetically induced transparency in cold atoms. Backward-wave, phase-matched difference-frequency conversion is achieved at optical powers of a few nanowatts and at energies of less than a picojoule.

DOI: 10.1103/PhysRevLett.93.183601 PACS numbers: 42.50.Gy, 32.80.–t, 42.65.Ky, 42.65.Lm

It is well known that nonlinear optical processes can be resonantly enhanced with electromagnetically induced transparency (EIT) [1] by simultaneously creating a destructive interference in absorption and a constructive interference in the nonlinear susceptibility [2]. This enhancement is greater in cold atoms where observable linewidths are close to natural linewidths. In this Letter, we demonstrate the first four-wave mixing experiment with EIT in cold atoms. Phase-matched frequency conversion with an efficiency of 10^{-4} is observed at pump energies of less than a picojoule. We use a backward-wave geometry, where weak Stokes and anti-Stokes fields counterpropagate through an optically thick atomic medium.

Our work builds on the ideas of nonlinear frequency conversion using EIT in double-Λ atomic systems [3–5]. Of special interest to this Letter is a backward-wave geometry where photons can be generated against a dark background. This configuration was demonstrated in an atomic medium by Hemmer *et al.* [6] using pump intensities of several watts/cm^2 and was brought to mirrorless oscillation with a few microwatts of pump power by Zibrov *et al.* [7]. Although there has been substantial work over the last decade on the subject of laser cooling and trapping of atoms, there have been relatively few studies of nonlinear processes in cold atoms. Previous demonstrations of nonlinear optical processes in cold atoms without EIT include multiwave mixing in an optical lattice [8] and phase conjugation [9], while the set of experiments using both EIT and cold atoms consists of quantum interference switching [10,11] and the giant Kerr nonlinearity [12].

The relevant ^{87}Rb energy levels for the double-Λ system of this experiment are shown in Fig. 1. A coupling laser of angular frequency ω_c, tuned to the $|2\rangle \rightarrow |3\rangle$ transition, sets up a quantum interference and provides transparency for an anti-Stokes laser. The magnitude of the coupling laser, together with the optical depth of the atomic medium, control the bandwidth of the transmission window for the applied anti-Stokes laser. The anti-Stokes and coupling lasers establish a spin wave of defined wave vector and phase. A pump laser of frequency ω_p, detuned from the $|1\rangle \rightarrow |4\rangle$ resonance in order to eliminate absorptive losses, mixes with the spin wave to produce a traveling wave dipole moment at the Stokes frequency ω_S. Together, these frequencies satisfy energy conservation $\omega_S = \omega_p + \omega_c - \omega_{AS}$.

Transparency at the anti-Stokes frequency is obtained when the square of the coupling laser Rabi frequency Ω_c is greater than the product of the decay from state $|3\rangle$ times the dephasing rate of the $|1\rangle \rightarrow |2\rangle$ transition [1]. It may then be shown that the ratio of the generation efficiency of an EIT process as compared to a resonant, conventional nonlinear optical process is the square of the optical depth ($\mathcal{N}\sigma L$). Also, EIT allows the generation of photons which are exactly at line center of a resonant transition; this is likely to be of importance for transmission of quantum information.

We proceed with a calculation of the line shape and generation efficiency of the backward-wave system of Fig. 1. Assuming that the coupling and the pump lasers are not depleted in the mixing process, the coupled equations in the slowly varying envelope approximation for the Stokes and anti-Stokes electric fields are

$$-\frac{\partial E_S^*}{\partial z} + \left(g_S - i\frac{\Delta k}{2}\right)E_S^* = \kappa_S E_{AS}$$
$$\frac{\partial E_{AS}}{\partial z} + \left(\alpha_{AS} - i\frac{\Delta k}{2}\right)E_{AS} = \kappa_{AS} E_S^*. \quad (1)$$

We note that this system exhibits two types of gain which we may term as Raman and parametric. The Raman gain g_S has a linewidth of $\sim 2|\Omega_c|$ and does not involve phase matching. The parametric gain, denoted by constants κ_{AS} and κ_S, results from the phase-matched interaction of the pump, Stokes, and coupling lasers with the anti-Stokes

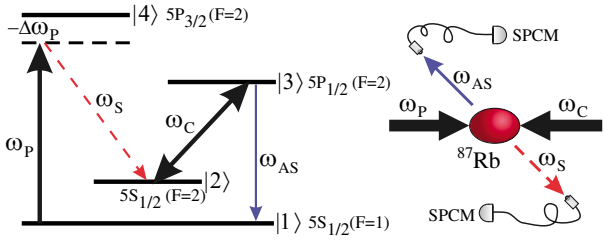

FIG. 1 (color online). Backward-wave four-wave mixing in a prototype, four-level system. In the presence of strong pump and coupling lasers, a weak anti-Stokes laser generates a counterpropagating, phase-matched Stokes beam.

waves. At a small density-length product $\mathcal{N}L$, the Raman gain varies as $\mathcal{N}L$, and the parametric gain varies as $(\mathcal{N}L)^2$. The absorption profile of the anti-Stokes laser is determined by α_{AS}. The geometrical phase mismatch $\Delta k = (\vec{k}_{AS} - \vec{k}_C + \vec{k}_S - \vec{k}_P) \cdot \hat{z}$ is taken along the propagation direction of the anti-Stokes beam.

The constants of the left-hand side of Eq. (1) may be determined from the linear susceptibilities χ_i where $g_S = -\omega_S/(2c) \times \mathrm{Im}[\chi_S^*]$ and $\alpha_{AS} = -\omega_{AS}/(2c) \times \mathrm{Im}[\chi_{AS}]$. Assuming the pumping field is sufficiently weak such that the atomic population remains primarily in the ground state $|1\rangle$, the linear susceptibilities at the Stokes and the anti-Stokes frequencies are

$$\chi_S^* = \frac{-c\mathcal{N}\sigma_{24}\gamma_{24}(\delta\omega + i\gamma_{13})}{|\Omega_c|^2 - 4(\delta\omega - i\gamma_{13})(\delta\omega - i\gamma_{12})} \times \left[\frac{|\Omega_p|^2}{\omega_p(\Delta\omega_{14}^2 + \gamma_{14}^2)}\right] \tag{2}$$

$$\chi_{AS} = \frac{4c\mathcal{N}\sigma\gamma_{13}(\delta\omega - i\gamma_{12})}{[|\Omega_c|^2 - 4(\delta\omega - i\gamma_{13})(\delta\omega - i\gamma_{12})]\omega_{AS}}.$$

The quantities $\Omega_p = \mu_{14}E_p/\hbar$ and $\Omega_c = \mu_{23}E_c/\hbar$ are the magnitudes of the Rabi frequencies of the pump and coupling lasers, μ_{ij} are the matrix elements, $\sigma_{ij} = \mu_{ij}^2\omega_{ij}/(c\epsilon_0\hbar\gamma_{ij})$ are absorption cross sections, γ_{ij} are dephasing rates, $\delta\omega = \omega_{AS} - (\omega_3 - \omega_1)$ is the detuning of the anti-Stokes frequency from the $|1\rangle \rightarrow |3\rangle$ transition, $\Delta\omega_{14} = \omega_p - (\omega_4 - \omega_1)$ is the detuning of the pump from the $|1\rangle \rightarrow |4\rangle$ transition, and $\mathcal{N}$ is the density of the atomic sample. The k-vector mismatch is taken in the atomic medium such that $k_i = (1 + \beta_i)\omega_i/c$ where β_i are the phase shifts relative to vacuum. Because of the steep EIT dispersion profile, the non-negligible phase shift at the anti-Stokes frequency is $\beta_{AS} = \omega_{AS}/(2c) \times \mathrm{Re}[\chi_{AS}]$; all other indices of refraction are taken as unity.

The parametric gain constants of the right-hand side of Eq. (1) are

$$\kappa_S = \frac{i\mathcal{N}\sqrt{\sigma_{13}\gamma_{13}\sigma_{24}\gamma_{24}}}{|\Omega_c|^2 - 4(\delta\omega - i\gamma_{13})(\delta\omega - i\gamma_{12})} \frac{\Omega_p^*\Omega_c^*}{2\Delta\tilde{\omega}_{14}}$$

$$\kappa_{AS} = \frac{-i\mathcal{N}\sqrt{\sigma_{13}\gamma_{13}\sigma_{24}\gamma_{24}}}{|\Omega_c|^2 - 4(\delta\omega - i\gamma_{13})(\delta\omega - i\gamma_{12})} \frac{\Omega_p\Omega_c}{2\Delta\tilde{\omega}_{14}^*} \tag{3}$$

where complex pump detuning is defined as $\Delta\tilde{\omega}_{14} = \Delta\omega_{14} - i\gamma_{14}$. The solution of Eq. (1) determines the conversion efficiency of the the anti-Stokes beam at $z = 0$ into the counterpropagating Stokes beam at $z = 0$:

$$\epsilon_S = \frac{P_S(z=0)}{P_{AS}(z=0)} = \left| \frac{2\kappa_{AS}}{q + \coth[\frac{L}{2}\sqrt{q^2 - 4\kappa_{AS}\kappa_S}]\sqrt{q^2 - 4\kappa_{AS}\kappa_S}} \right|^2 \tag{4}$$

where $q \equiv \alpha_{AS} + g_S + i\Delta k_z$.

Frequency conversion is performed in a gas of cold ^{87}Rb atoms which are cooled and trapped in a dark magneto-optical trap (MOT). A Ti:sapphire laser, which is locked 20 MHz below the $5S_{1/2}(F = 2) \rightarrow 5P_{3/2}(F' = 3)$ transition, supplies three, perpendicular, retro-reflected, trapping beams. Each of these beams has a $1/e$ diameter of 2 cm and a power of 65 mW. A repumping (extended-cavity, diode) laser locked to the $5S_{1/2}(F = 1) \rightarrow 5P_{3/2}(F' = 2)$ transition recycles atoms from the $5S_{1/2}(F = 1)$ level. Throughout the experiment, we maintain a Rb vapor pressure of $\sim 10^{-9}$ torr in a 10-port, stainless-steel vacuum chamber. The atoms are loaded into the MOT with a quadrupole magnetic field gradient of 6 G/cm for 4 s. Three pairs of Helmholtz coils zero the background magnetic field. In order to compress the cloud, the magnetic field gradient is ramped to 20 G/cm, and the trapping laser is detuned 50 MHz below resonance for 30 ms. By shuttering the repumping laser for 700 μs after initial compression, the atoms are shelved into the dark, $F = 1$, ground level. The resulting atom cloud is 1.5 mm in diameter and has $\sim 5 \times 10^8$ atoms with an estimated temperature of ~ 150 μK. At this temperature, the effect of Doppler broadening on EIT is negligible. The optical thickness of the sample was measured by absorption to be $\mathcal{N}\sigma_{13}L \sim 13$. The experiment is performed in a 200 μs window 50 μs after shutting off the trapping beams. This cooling, trapping, and data-collection process is cycled at 0.2 Hz.

All of the lasers used in the four-wave mixing experiment are external-cavity diode lasers which are spatially filtered in single-mode fibers. The coupling and anti-Stokes lasers, with linewidths <300 kHz, are phase and frequency locked [13] on the D_1 line to a reference laser (which is frequency-stabilized to a saturated-absorption ^{85}Rb line). The coupling laser seeds a taper amplifier whose output is spatially filtered using a polarization-maintaining fiber. The pump laser is frequency stabilized on the D_2 line of Rb, and its wavelength can be locked either to $|1\rangle \rightarrow |4\rangle$ for difference-frequency generation or to $|2\rangle \rightarrow |4\rangle$ for sum-frequency alignment.

In order to overlap the anti-Stokes and Stokes lasers in the atomic cloud, we align these lasers to be collinear and counterpropagating along the z axis. Because the Stokes and anti-Stokes waves have different frequencies, it is not possible to have exact phase matching in the backward configuration. We choose the angle between the z axis and the axis defined by the pump and coupling lasers to be $\sim 2°$ which provides spatial separation between the weak anti-Stokes/Stokes photons and the two strong beams. This choice does not affect the Stokes generation since the efficiency as given in Eq. (4) is flat at such small angles. The resulting coherence length along the z axis is much longer than the 1.5 mm atomic cloud length. Similarly, the coherence length in the perpendicular direction is much longer than the anti-Stokes and Stokes lasers' 80 μm beam diameters.

As shown in Fig. 1, anti-Stokes and Stokes laser beams are counterpropagating through two single-mode fibers separated by 0.5 m. These fibers are aligned to each other through the atom cloud with a measured fiber coupling efficiency of 80%. To ensure that the Stokes beam will be generated into an optical fiber, we use a sum-frequency alignment process in which input coupling, Stokes and anti-Stokes lasers generate a beam at the pump laser wavelength ($|1\rangle \rightarrow |4\rangle$ transition). The input pump laser in the difference-frequency experiment is aligned such that it overlaps the generated, sum frequency, pump beam. This procedure guarantees that the difference-frequency Stokes photons counterpropagate with respect to the anti-Stokes photons.

Figure 2 shows anti-Stokes transmission in the absence of pump and coupling lasers. The power in the anti-Stokes beam is less then a picowatt in a 200 μs pulse, and transmission is measured using a fiber-coupled single photon-counting module (Perkin-Elmer SPCM-AQR). Each data point is an average over ten atom clouds. Using a least-squares fit, the total optical depth of the atomic sample is $\mathcal{N}\sigma_{13}L = 13.3 \pm 0.4$.

The addition of a coupling laser creates a destructive quantum interference in absorption, and the anti-Stokes laser has nearly 100% transmission at the line center. The observed EIT line profile also is shown in Fig. 2. Anti-Stokes and coupling lasers have the same circular polarization. Because the hyperfine levels of Rb have many Zeeman sublevels, laser polarizations must be aligned correctly in order to create parallel channels for EIT [11]. Each EIT channel is described by a three-level system, and the total susceptibility for the system of parallel channels is the sum of each single channel susceptibility. If, however, there is coupling between different channels (for example, due to incorrect laser polarization), the channels are no longer independent, and the anti-Stokes laser experiences absorptive loss. Experimentally, we observe a dramatic loss in transparency (as well as in Stokes generation) when the polarization of the anti-Stokes laser mixes the channels.

The magnitude of the parametric nonlinearity is inversely proportional to the coupling laser Rabi frequency. Consequently, Ω_c should be as weak as possible without loss of transparency. Due to an experimentally observed dephasing rate γ_{12}, absorption of the anti-Stokes laser in the transparency window occurs at coupling laser Rabi frequency on the order of the natural linewidth of the Rb D_1 line ($\Gamma_3 = 5.9$ MHz). We observe an unexplained increase of γ_{12} (as measured from a fit of the EIT, transmission profile) when Ω_c is decreased. Using a least-squares fit, as shown by the solid line in Fig. 2, the Rabi frequency of the coupling laser is $\Omega_c = (2.5 \pm 0.1)\Gamma_3$. In this regime, absorption of the anti-Stokes laser on resonance is negligible.

The intensity of the generated Stokes field depends strongly on the detuning of the pump beam as seen in Fig. 3. As the pump is tuned close to resonance, the nonlinearity is increased, and the efficiency of generated Stokes photons is increased. The data are taken in a regime where there is small absorption of the pump beam ($\Omega_p/\Delta\omega_p \ll 1$). This solid line is the predicted efficiency of the parametric process vertically scaled at one point. The theory curve is based on a four-level system while the actual atomic sample has 12 different Zeeman sublevels (3 parallel channels with four levels). The four-level theory presumes the initial condition of equal populations in each ground hyperfine state whereas actual trapped-atom populations may deviate from this assumption [14]. Differences in population change the weight of matrix elements in each channel and thus also the magnitude of the predicted efficiency.

Figure 4 shows efficiency of the generated Stokes power as a function of the anti-Stokes detuning with the pump laser detuned by $4\Gamma_3$. The solid curve shown

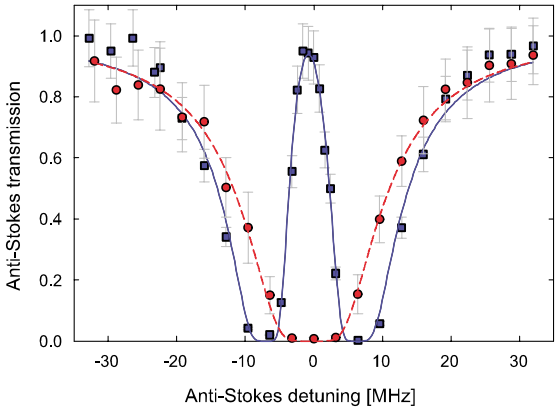

FIG. 2 (color online). Anti-Stokes laser transmission in the absence of coupling and pump lasers (red circle) and transmission in the presence of the coupling laser (blue square). Experimental parameters $\mathcal{N}\sigma_{13}L = 13.4 \pm 0.6$ and $\Omega_c = (2.5 \pm 0.1)\Gamma_3$ are determined from a least-squares fit.

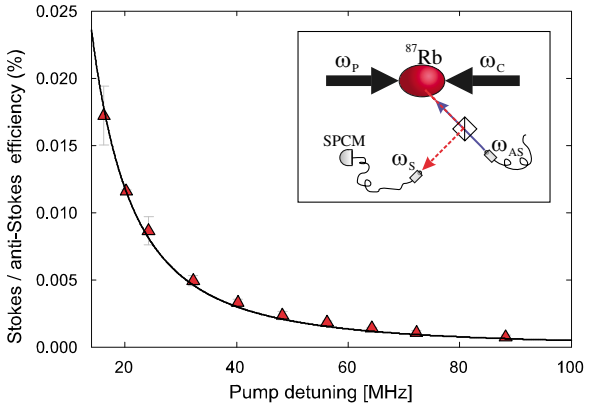

FIG. 3 (color online). Efficiency of generated Stokes beam to anti-Stokes beam (red triangle) as a function of pump laser detuning (or effectively, the pump laser power). The theoretical prediction (solid line) is vertically scaled down by 20%. Inset shows optical layout for detection of generated Stokes photons.

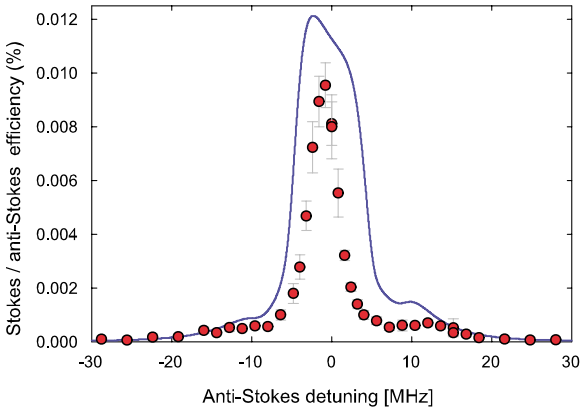

FIG. 4 (color online). Efficiency of Stokes photons to anti-Stokes photons as a function of anti-Stokes laser detuning. Pump laser, with Rabi frequency $\Omega_p = 0.04\Gamma_3$, is detuned by $\Delta\omega_p = 4\Gamma_4$. Coupling laser Rabi frequency is $\Omega_c = 2.5\Gamma_3$. Theory curve (solid line) is plotted over the experimental results (red circle), with no free parameters.

in the plot is a theoretical prediction of Eq. (4) as discussed above using no free parameters. Total pump and anti-Stokes laser powers for Figs. 3 and 4 are 400 nW and 150 nW, respectively. Allowing for spatial beam overlap of the 80 μm anti-Stokes and 1.2 mm pump lasers, the pump power actually used in frequency conversion is four nW. The experiment is performed with 200 μs pulses; therefore, the energy of the pump laser is less than a picojoule, and energy per area is less than a single photon per atomic cross section for a conversion efficiency of 10^{-4}. To our knowledge, this is the lowest light-level frequency mixing reported up to date.

Dependence of the efficiency of the generated Stokes power on the density-length product of the atomic sample is shown in Fig. 5. Here, after trapping is turned off, the atomic sample expands before the difference-frequency experiment is performed. By controlling the duration of this expansion, the optical depth may be varied. From Eq. (4), we expect efficiency to scale quadratically with density-length ($\mathcal{N}L$) product. The observed data follow this quadratic trend.

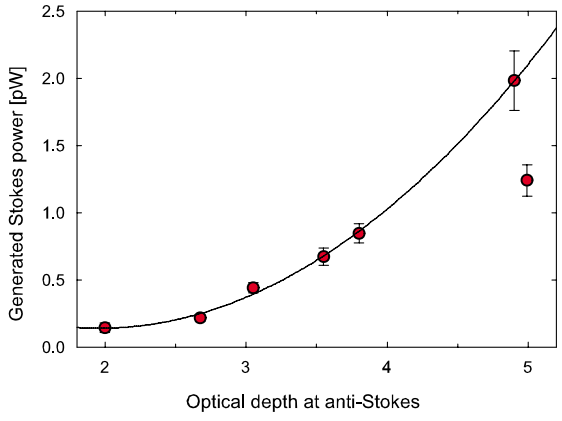

FIG. 5 (color online). Stokes efficiency (red circle) as a function of the optical depth ($\mathcal{N}\sigma_{13}L$) at the anti-Stokes laser.

If in our four-level system shown in Fig. 1, one applies only counterpropagating coupling and pump lasers, the system will spontaneously emit pairs of photons at the Stokes and anti-Stokes frequencies [15]. The noncollinear, backward-wave geometry assures that both photons will be emitted against a dark background, and the photons may be directly detected without additional filtering. The bandwidth of the emitted photons can be controlled by the density-length product. For our experimental conditions, the bandwidth is ~5 MHz with a corresponding coherence length of 60 m, which is 5 orders of magnitude longer than the typical lengths of paired photons created using parametric down conversion.

This work was supported by the U.S. Air Force Office of Scientific Research, the U.S. Army Research Office, Multidisciplinary Research Initiative Program, the U.S. Office of Naval Research, and the Fannie and John Hertz Foundation (D. A. B.).

*Electronic address: braje@stanfordalumni.org

[1] S. E. Harris, Phys. Today **50**, No. 7, 36 (1997); J. P. Marangos, J. Mod. Opt. **45**, 471 (1998); R. W. Boyd and D. J. Gauthier, *Progress in Optics* (Elsevier, New York, 2002), Vol. 43, p. 497.
[2] S. E. Harris, J. E. Field, and A. Imamoglu, Phys. Rev. Lett. **64**, 1107 (1990); S. E. Harris and Lene Vestergaard Hau, Phys. Rev. Lett. **82**, 4611 (1999).
[3] Maneesh Jain *et al.*, Phys. Rev. Lett. **77**, 4326 (1996).
[4] S. Babin *et al.*, Opt. Lett. **21**, 1186 (1996).
[5] B. Lü, W. H. Burkett, and M. Xiao, Opt. Lett. **23**, 804 (1998).
[6] P. R. Hemmer *et al.*, Opt. Lett. **20**, 982 (1995).
[7] A. S. Zibrov, M. D. Lukin, and M. O. Scully, Phys. Rev. Lett. **83**, 4049 (1999); M. Fleischhauer *et al.*, Phys. Rev. Lett. **84**, 3558 (2000).
[8] A. Hemmerich, M. Weidemüller, and T. Hänsch, Europhys. Lett. **27**, 427 (1994).
[9] S. Barreiro and J. W. R. Tabosa, Phys. Rev. Lett. **90**, 133001 (2003); Yoshio Torii *et al.*, Prog. Cryst. Growth Charact. Mater. **33**, 413 (1996).
[10] Min Yan, Edward G. Rickey, and Yifu Zhu, Phys. Rev. A **64**, 041801(R) (2001).
[11] D. A. Braje *et al.*, Phys. Rev. A **68**, 041801(R) (2003).
[12] H. Kang and Yifu Zhu, Phys. Rev. Lett. **91**, 093601 (2003).
[13] M. Prevedelli, T. Freegarde, and T. W. Hänsch, Appl. Phys. B **60**, S241 (1995).
[14] M. Kasevich *et al.*, Phys. Rev. Lett. **63**, 612 (1989); D. Grison *et al.*, Europhys. Lett. **15**, 149 (1991).
[15] C. H. van der Wal *et al.*, Science **301**, 196 (2003); A. Kuzmich *et al.*, Nature (London) **423**, 731 (2003).